Constructing host-σ-guest structure to optimize the efficiency of nondoped solution-processed OLED

Dan Liu, [†a] Meng Zhang, [†a] Haowen Chen, [a] Daiyu Ma, [a] Wenwen Tian, [a] Kaiyong Sun, [a, b] Wei Jiang, [*a] and Yueming Sun, [*a]

[a]Jiangsu Province Hi-Tech Key Laboratory for Bio-Medical Research, Jiangsu Engineering Laboratory of Smart Carbon-Rich Materials and Device, School of Chemistry and Chemical Engineering, Southeast University, Nanjing, 211189, China
[b]School of Chemistry and Chemical Engineering, Yancheng Institute of Technology, Yancheng, Jiangsu 224051, China

Email: jiangw@seu.edu.cn (Wei Jiang) sun@seu.edu.cn (Yueming Sun)

Keywords: Thermally activated Delayed Fluorescence (TADF), Aggregation-Induced Emission (AIE) Organic light-emitting diodes (OLED), host-σ-guest structure.

Table of Contents

General information

All solvents and materials were used as received from commercial sources without further purification. ^{1}H NMR and ^{13}C HMR spectra were recorded on a BRUKER AMX 600-MHz instrument. Elemental analysis was determined by an Elementar Vario EL CHN elemental analyzer. Mass spectrometry was performed with a Thermo Electron Corporation Finnigan LTQ mass spectrometer. The UV-Vis absorption spectra of the compounds were measured by SHIMADZU UV-2450. The photoluminescence emission spectra were recorded on HORIBA FLUOROMAX-4. Thermogravimetric analysis (TGA) and Differential scanning calorimetry (DSC) curves were recorded with a Netzsch simultaneous thermal analyzer (STA) system (STA 409PC) and DSC 2910 modulated calorimeter under a dry nitrogen gas flow at a heating rate of 10°C min^{-1}. Cyclic voltammetry (CV) was performed on a CHI750C voltammetric analyzer in a typical three-electrode cell with a platinum plate working electrode, a platinum wire counter electrode and a silver wire reference electrode. The supporting electrolyte was tetrabutylammonium hexafluorophosphate (0.1M) and ferrocene was selected as the internal standard. AFM (Seiko Instruments, SPA-400) was used to measure the film surface morphology. The measured pure films were formed by spin-coating and the solvent is 1,2-dichloroethane. The optimized structure was calculated by Gaussian09 at the B3LYP functional with 6-31G(d) basis sets. The molecular orbitals were visualized using Gaussview 5.0.

The Lippert-Mataga model is extimated according to equation

$$hc(v_a - v_f) = hc(v_a^0 - v_f^0) + \frac{2(\mu_e - \mu_g)^2}{a_0^3} f(\varepsilon,n)$$

or

$$\mu_e = \mu_g + \left\{ \frac{hca_0^3}{2} \cdot \left[\frac{d(v_a - v_f)}{df(\varepsilon,n)} \right] \right\}^{1/2}$$

where μ_e is the dipole moment of excited state, μ_g is the dipole moment of ground state, h is the Plank constant, c is the light speed in vacuum, a_0 is the solvent Onsager cavity radius, $v_a - v_f$ is the Stokes shift, $f(\varepsilon,n)$ is the orientational polarizability of solvents and $f(\varepsilon,n) = \left[\frac{\varepsilon - 1}{2\varepsilon + 1} - \frac{n^2 - 1}{2n^2 + 1} \right]$. ε is the solvent dielectric constant and n is the solvent refractive index. μ_g was estimated by DFT. The differential $\frac{d(v_a - v_f)}{df(\varepsilon,n)}$ can be estimated based on the solvatochromic experiment data. The selection of emission peak for these compounds in various solvents is based on maximum intensity in the total spectral range, which corresponds to the dominant-character (LE or CT) in S$_1$ state.

To fabricate the nondoped solution-processed OLEDs, a 40 nm thick poly(3,4-ethylenedioxythiophene): poly(styrenesulfonate) (PEDOT: PSS) film was first spin-coated on the pre-cleaned ITO glass substrates with 3000 rpm rotation speed and baked at 150 ℃ for 10 min. Subsequently, a 40 nm thick PO-T2T layer was evaporated at a rate of 1 Å/s as the electron transporting layer. Finally, 2 nm thick Cs_2CO_3 and 100 nm thick Al layers were evaporated at a rate of 2 Å/s as the cathode. The EL spectra and CIE coordinates were measured using a PR655 spectra colorimeter. The current density-voltage and brightness-voltage curves of the devices were plotted using a Keithley 2400 source meter calibrated by a silicon photodiode. All the measurements were carried out at room temperature with no protective encapsulation. The EQE was calculated from the brightness, current density and EL spectrum assuming a Lambertian distribution.

Materials and synthesis

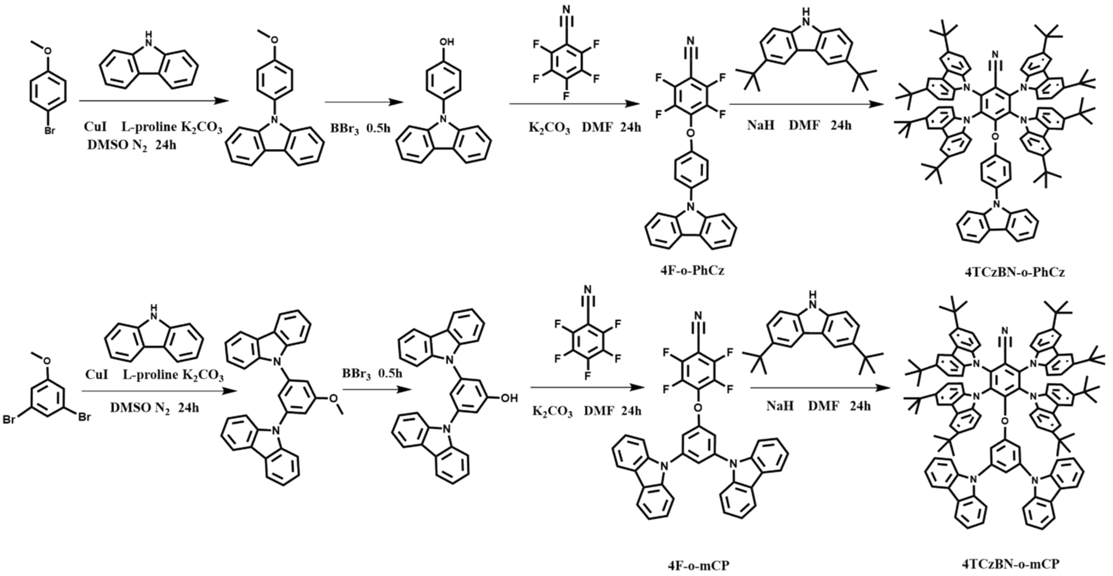

Scheme 1 Synthetic routes of 4TCzBN-o-PhCz and 4TCzBN-o-mCP.

All chemicals and reagents were used as received from commercial sources without further purification. Solvents for chemical synthesis were purified according to the standard procedures. The manipulations involving air-sensitive reagents were performed under a dry nitrogen atmosphere. 9-(4-methoxyphenyl)-9H-carbazole, 4-(9H-carbazol-9-yl)phenol, 9,9'-(5-methoxy-1,3-phenylene)bis(9H-carbazole), 3,5-di(9H-carbazol-9-yl)phenol and 2,3,5,6-tetrakis(3,6-di-tert-butyl-9H-carbazol-9-yl)benzonitrilee (4TCzBN) were prepared according to literature procedure[1-5].

(1) 4-(4-(9H-carbazol-9-yl)phenoxy)-2,3,5,6-tetrafluorobenzonitrile (4F-o-PhCz)

To a stirring solution of 4-(9H-carbazol-9-yl)phenol (1 g, 3.9 mmol) and potassium carbonate (K_2CO_3 (1.6 g, 11.6 mmol)) in DMF (20 mL), and 2,3,4,5,6-pentafluorobenzonitrile (0.89 g, 4.6 mmol) were added sequentially into a round-bottomed flask. And the mixture was refluxed for 12 h. Then the resulting mixture was placed into 100 mL saturated salt solution, and the desired product was extracted with dichloromethane (3×50 mL). The organic layer was then separated, dried over sodium sulfate (Na_2SO_4), filtered and evaporated under reduced pressure to give a crude product which was further purified by column chromatography using petroleum ether/dichloromethane (3/1, v/v) to obtain the final product (1.1 g, 66%). ^{1}H NMR (600 MHz, $CDCl_3$, δ): 8.15 (d, J = 7.8 Hz, 2H), 7.58 (d, J = 9 Hz, 2H), 7.42-7.41 (t, J = 6.6 Hz, 2 H), 7.35 (d, J = 8.4 Hz, 2 H), 7.31 (t, J = 8.4 Hz, 2 H), 7.25 (d, J = 9 Hz, 2 H). LC/MS [m/z]: calcd for $C_{25}H_{12}F_4N_2O$, 432.09; found, 432.03. Anal. Calcd for $C_{25}H_{12}F_4N_2O$: C, 69.45; H, 2.80; F, 17.58; N, 6.48; O, 3.70. Found: C, 69.23; H, 2.85; N, 6.45.

(2) 4-(3,5-di(9H-carbazol-9-yl)phenoxy)-2,3,5,6-tetrafluorobenzonitrile (4F-o-mCP)

The intermediate 4F-o-mCP was synthesized in a fashion similar to that for 4F-o-PhCz but using

3,5-di(9H-carbazol-9-yl)phenol (1.64 g, 3.9 mmol), potassium carbonate (K_2CO_3 (1.6 g, 11.6 mmol)) and 2,3,4,5,6-pentafluorobenzonitrile (0.89 g, 4.6 mmol). The product was obtained as a white solid (1.8 g, 78 %). ^{1}H NMR (600 MHz, $CDCl_3$, δ): 8.15 (d, J = 7.8 Hz, 4H), 8.01 (s, 1 H), 7.72 (s, 1 H), 7.55 (d, J = 7.8 Hz, 3 H), 7.47 (t, J = 8.4 Hz, 4 H), 7.34 (t, J = 7.8 Hz, 6 H). LC/MS [m/z]: calcd for $C_{25}H_{12}F_4N_2O$, 597.57; found, 597.55. Anal. Calcd for $C_{37}H_{19}F_4N_3O$: C, 74.37; H, 3.20; F, 12.72; N, 7.03; O, 2.68 Found: C, 74.32; H, 3.12; N, 7.12.

(3) 4-(4-(9H-carbazol-9-yl)phenoxy)-2,3,5,6-tetrakis(3,6-di-tert-butyl-9H-carbazol-9-yl)benzonitrilee (4TCzBN-o-PhCz)

Under nitrogen atmosphere, 3,6-di-tert-butyl-9H-carbazole (1 g, 3.6 mmol) in anhydrous THF (20 mL) was added dropwise into an anhydrous THF (10 mL) solution containing NaH (0.86 g, 35.8 mmol) and stirred for 30 min. Then, 4-(4-(9H-carbazol-9-yl)phenoxy)-2,3,5,6-tetrafluorobenzonitrile (4F-o-PhCz, 0.26 g, 0.6 mmol) was added slowly into the mixtures. Then the solution was stirred for 24 h at room temperature. After that, 250 mL of water was added into the solution and the mixture was extracted with CH_2Cl_2 three times. The combined organic layer was dried with anhydrous MgSO4 and the solvent was removed under vacuum. The precipitate was purified by column chromatography on silica gel, resulted in the yellow green product (0.5 g, 57%).

^{1}H NMR (600 MHz, $CDCl_3$, δ): 7.90 (d, 10.2 Hz, 2 H), 7.58 (s, 4 H), 7.53 (s, 4 H), 7.18 (d, 8.4 Hz, 4 H), 7.07-6.99 (m, 15 H), 6.92 (d, 8.4 Hz, 1 H), 6.61 (d, 9.0 Hz, 2 H), 6.43-6.40 (m, 4 H), 1.39 (d, 13.2 Hz, 72 H). ^{13}C NMR (150 MHz, $CDCl_3$, δ): 142.93, 142.40, 139.58, 136.19, 135.88, 126.49, 123.64, 121.97, 118.83, 116.01, 114.46, 108.74, 108.44, 108.20. 33.54, 30.88. MS (MALDI-TOF) [m/z]: calcd for $C_{105}H_{108}N_6O$, 1469.86; found, 1469.862. Anal. Calcd for $C_{105}H_{108}N_6O$: C, 85.79; H, 7.41; N, 5.72; O, 1.09 Found: C, 85.72; H, 7.52; N, 5.74.

(4) 4-(3,5-di(9H-carbazol-9-yl)phenoxy)-2,3,5,6- tetrakis(3,6-di-tert-butyl-9H-carbazol-9-yl)benzonitrilee (4TCzBN-o-mCP)

The emitter was synthesized in a fashion similar to that for 4TCzBN-o-PhCz but using 3,6-di-tert-butyl-9H-carbazole (1 g, 3.6 mmol), NaH (0.86 g, 35.8 mmol) and 4-(3,5-di(9H-carbazol-9-yl)phenoxy)-2,3,5,6-tetrafluorobenzonitrile (0.35 g, 0.6 mmol). The product was obtained as a yellow green solid (0.6 g, 61 %).^{1}H NMR (600 MHz, $CDCl_3$, δ): 7.94 (d, J = 7.2 Hz, 5 H), 7.56 (d, J = 16.8 Hz, 10 H), 7.14 (m, 10 H), 7.04 (m, 10 H), 6.63 (s, 1 H), 6.54 (s, 2 H), 6.43 (d, J = 8.4 Hz, 5 H). 1.38 (s, 72 H). ^{13}C NMR (150 MHz, $CDCl_3$, δ): 157.51, 155.33, 142.96, 139.07, 138.90, 138.19, 136.02, 135.84, 128.47, 124.91, 123.10, 122.08, 121.96, 119.01, 118.80, 114.60, 114.50, 112.90, 112.65, 112.55, 108.93, 108.54, 108.42. 33.50, 30.87. MS (MALDI-TOF) [m/z]: calcd for $C_{117}H_{115}N_7O$, 1634.92; found, 1634.931. Anal. Calcd for $C_{117}H_{115}N_7O$: C, 85.79; H, 7.41; N, 5.72; O, 1.09 Found: C, 85.72; H, 7.52; N, 5.74.

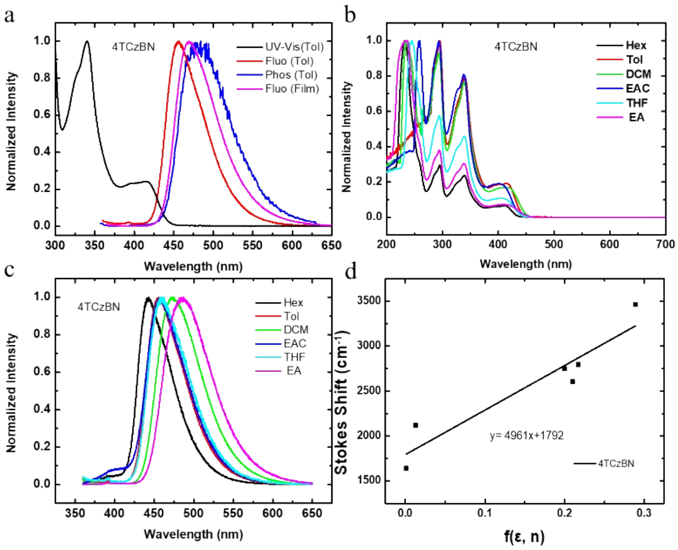

Figure S1. (a) The UV-Vis, Fluorescence and Phosphorescence spectra of 4TCzBN (b) Absorption spectra in solvents with different polarities (c) Fluorescence spectra in solvents with different polarities (d) The Lippert-Mataga curves in different orientation polarization of the solvent.

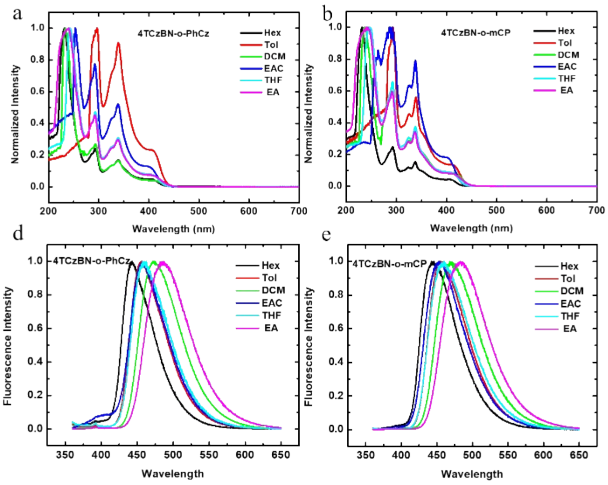

Figure S2. The absorption and photoluminescence spectra of 4TCzBN-o-PhCz and 4TCzBN-o-mCP in solvents of different polarities.

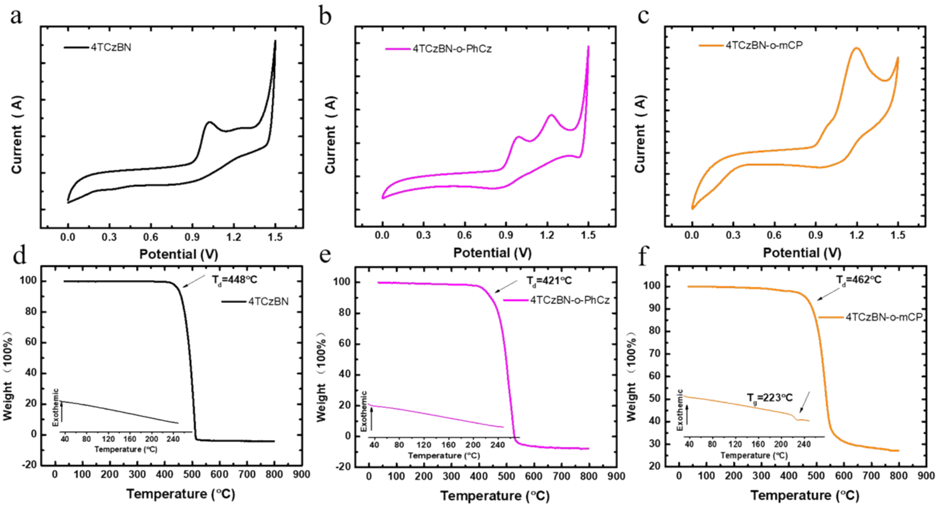

Figure S3. The oxidation reaction CV curves of 4TCzBN (a), 4TCzBN-o-PhCz (b) and 4TCzBN-o-mCP (c). The DSC and TGA thermograms of 4TCzBN (d), 4TCzBN-o-PhCz (e) and 4TCzBN-o-mCP (f).

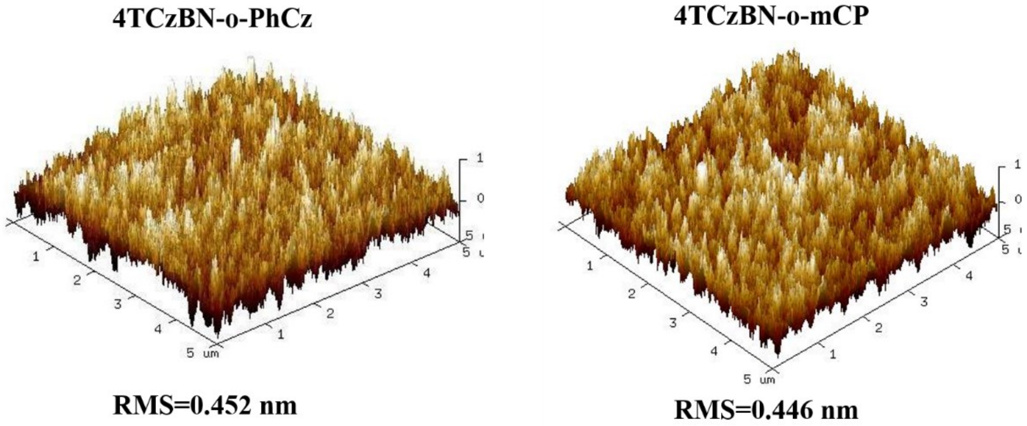

Figure S4. The AFM picture of 4TCzBN-o-PhCz and 4TCzBN-o-mCP.

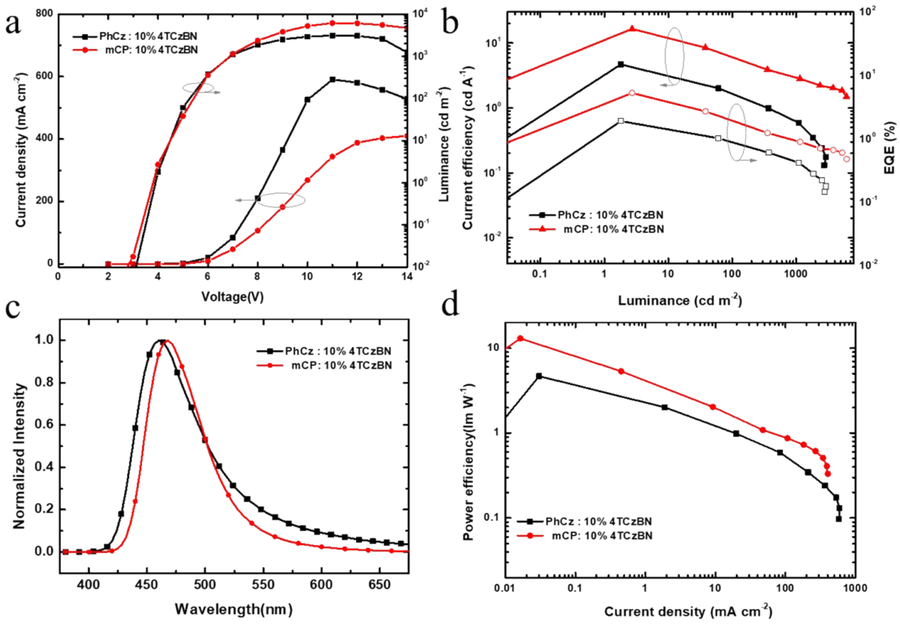

Figure S5. The device performances of doped OLEDs. (a) Current density-voltage-luminance (J-V-L) characteristic of device D-E. (b) current efficiencies versus brightness and the external quantum efficiency versus brightness. (c) electroluminescence spectra at 10 V. (d) power efficiency versus current density.

The doped solution-processed devices were fabricated with an architecture of ITO/PEDOT: PSS (40 nm)/PhCz: 10% 4TCzBN (Device D) or mCP: 10% 4TCzBN (Device E)/PO-T2T (40 nm)/Cs_2CO_3 (2 nm)/Al. The characteristics of the doped OLEDs were summarized in Table S4. Contrary to expectation, these doped devices using PhCz and mCP as hosts exhibited poorer device performances with 1.9% EQE and 5.3% EQE, respectively. This results are different from vacuum-evaporated OLEDs, which demonstrated more excellent performance in doped devices in general. In solution process, the morphology of films is significant for the fabrication of OLEDs. Because of poor film-forming ability and phase separation existed in PhCz and mCP doped films, the surface of the compounds exhibited a kind of aggregation and some pinholes (J. Mater. Chem., 2010,20, 6131-6137). This will lead to leakage currents and poor efficiency in solution-processed OLEDs. Therefore, this result is also consistent with the view that the molecular design of host-sigma-guest structure can reduce the phase separation, meanwhile improve the device performance.

Table S1. Calculated HOMO, LUMO, Bandgap, S_1, T_1, ΔE_{ST}, the oscillator strength (f) and dipole moment values from DFT and TD-DFT at B3LYP/6-31g(d) level.

Compounds	HOMO [eV]	LUMO [eV]	E_g [eV]	S_1 [eV]	T_1 [eV]	ΔE_{ST} [eV]	The oscillator strength(f)	The dipole moments in S_0 and S_1 states
4TCzBN	-5.25	-1.90	3.35	2.72	2.59	0.13	0.1072	3.41 D/2.42 D
4TCzBN-o-PhCz	-5.30	-1.92	3.38	2.75	2.64	0.11	0.1000	2.33 D/0.97 D
4TCzBN-o-mCP	-5.31	-1.94	3.37	2.74	2.63	0.11	0.0887	2.00 D/1.93 D

Table S2 Photophysical data of 4TCzBN, 4TCzBN-o-PhCz and 4TCzBN-o-mCP in solvents of different polarities.

Solvents	f(ε,n)	4TCzBN				4TCzBN-o-PhCz				4TCzBN-o-mCP			
		λ_{abs} (nm)	λ_{emi} (nm)	υ_a-υ_f (cm^{-1})	Dipole moment	λ_{abs} (nm)	λ_{emi} (nm)	υ_a-υ_f (cm^{-1})	Dipole moment	λ_{abs} (nm)	λemi (nm)	υ_a-υ_f (cm^{-1})	Dipole moment
Hexane	0.0012	413	443	1639.7	1.59 D	406	442	2006.1	1.62 D	410	445	1918.3	1.59 D
Toluene	0.013	415	455	2118.4		407	456	2640.2		415	456	2166.6	
Ethyl acetate	0.2	406	457	2748.7		402	457	2993.8		403	453	2738.8	
THF	0.21	410	459	2603.8		403	459	3027.4		412	459	2485.4	
Dichloromethane	0.217	417	472	2794.4		410	473	3248.6		411	470	3054.3	
Ethanol	0.289	416	487	3504.6		408	486	3933.7		412	483	3567.9	

Table S3. Photophysical characteristic and kinetic parameters of 4TCzBN-o-PhCz and 4TCzBN-o-mCP.

emitters	ϕ_{PL}(%) Film	τ_p(ns) R_p	τ_d(μs) R_d	k_r b) [10^5 s^{-1}]	k_{nr} b) [10^5 s^{-1}]	k_F c) [10^6 s^{-1}]	k_{IC} c) [10^6 s^{-1}]	k_{ISC} c) [10^7 s^{-1}]	k_{RISC} c) [10^6 s^{-1}]	Φ_{RISC}
4TCzBN-o-PhCz	39.4	287 16.1%	2.19, 83.9%	1.79	2.77	0.22	0.34	2.92	2.84	39.40
4TCzBN-o-mCP	60.8	388 11.5%	3.03, 88.5%	2.01	1.30	0.15	0.10	2.33	3.51	60.80

a) Measured in toluene at 300K and before (left) and after (right) N_2 bubbling. b) Calculated radiative decay rate k_r and nonradiative decay rate k_{nr} according to the equations: $\tau=1/(k_r+k_{nr})$, and $\phi_{PL}=k_r/(k_r+k_{nr})$. where τ is the total lifetimes of the transient and the delayed components, ϕ_{PL} is the PLQY of films. c) Calculated k_F, internal conversion decay rate k_{IC}, intersystem crossing decay rate k_{ISC} from S_1 to S_0 and the rate constant of reverse intersystem crossing process k_{RISC}. The detailed calculation formulas were shown in the supporting information.

Table S4 The summary of doped devices based on PhCz: 10% 4TCzBN and mCP: 10% 4TCzBN emitters.

Device	emitter	V_{on}^{a}	EL(nm)	CE_{max}^{b}	PE_{max}^{c}	EQE_{max}^{d}	L_{max}^{f}	CIE(x,y)^g
D	PhCz: 10% 4TCzBN	3.8	460	6.0	4.7	1.9	3100	(0.19,0.10)
E	mCP: 10% 4TCzBN	3.6	468	16.6	13.0	5.3	6200	(0.15,0.19)

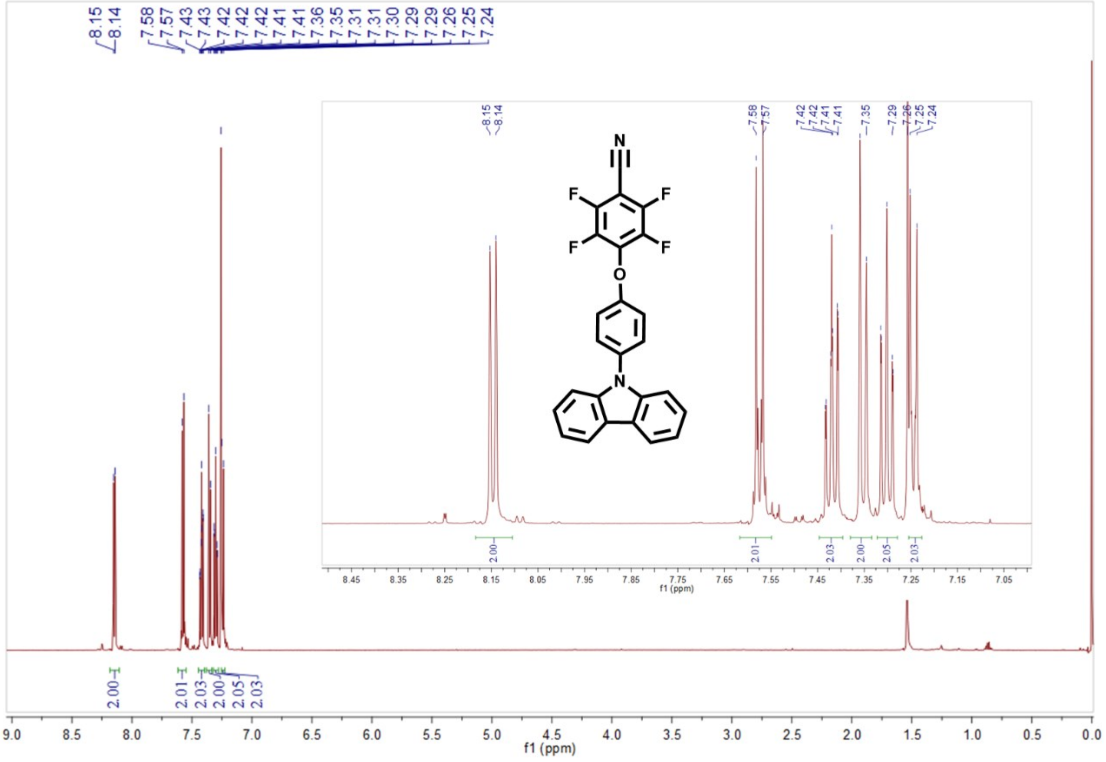

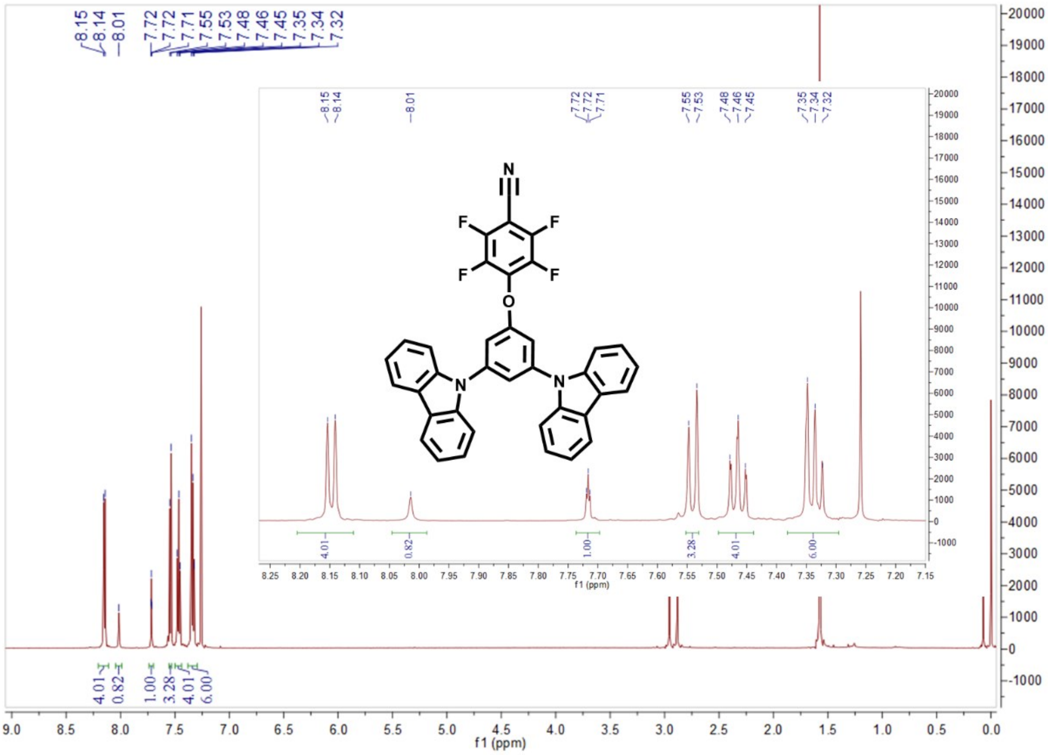
8.15
8.14
8.01
7.72
7.72
7.71
7.55
7.53
7.48
7.46
7.45
7.35
7.34
7.32
4.01
0.82
1.00
3.28
4.01
6.00
N
F
F
F
F
O
N
N
20000
19000
18000
17000
16000
15000
14000
13000
12000
11000
10000
9000
8000
7000
6000
5000
4000
3000
2000
1000
0
-1000
8.25 8.20 8.15 8.10 8.05 8.00 7.95 7.90 7.85 7.80 7.75 7.70 7.65 7.60 7.55 7.50 7.45 7.40 7.35 7.30 7.25 7.20 7.15
9.0 8.5 8.0 7.5 7.0 6.5 6.0 5.5 5.0 4.5 4.0 3.5 3.0 2.5 2.0 1.5 1.0 0.5 0.0
f1 (ppm)

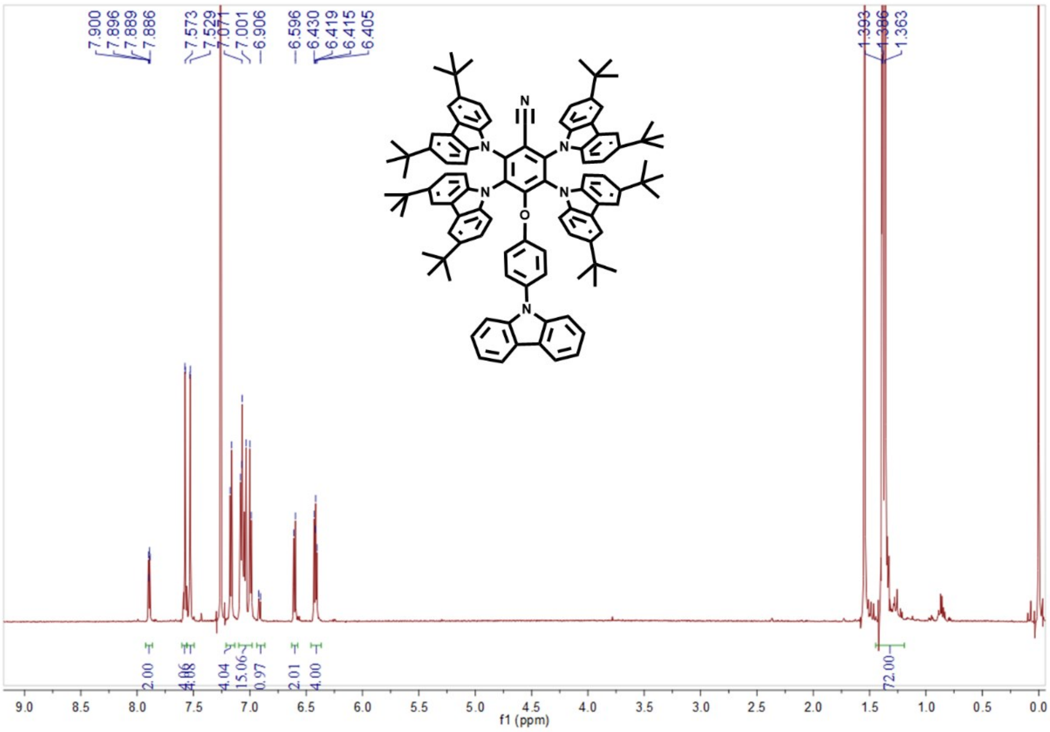
7.900
7.896
7.889
7.886
7.573
7.529
7.071
7.001
6.906
6.596
6.430
6.419
6.415
6.405
1.393
1.386
1.363
N
N
N
N
N
O
N
2.00
4.06
4.08
4.04
15.06
0.97
2.01
4.00
72.00
9.0 8.5 8.0 7.5 7.0 6.5 6.0 5.5 5.0 4.5 4.0 3.5 3.0 2.5 2.0 1.5 1.0 0.5 0.0
f1 (ppm)

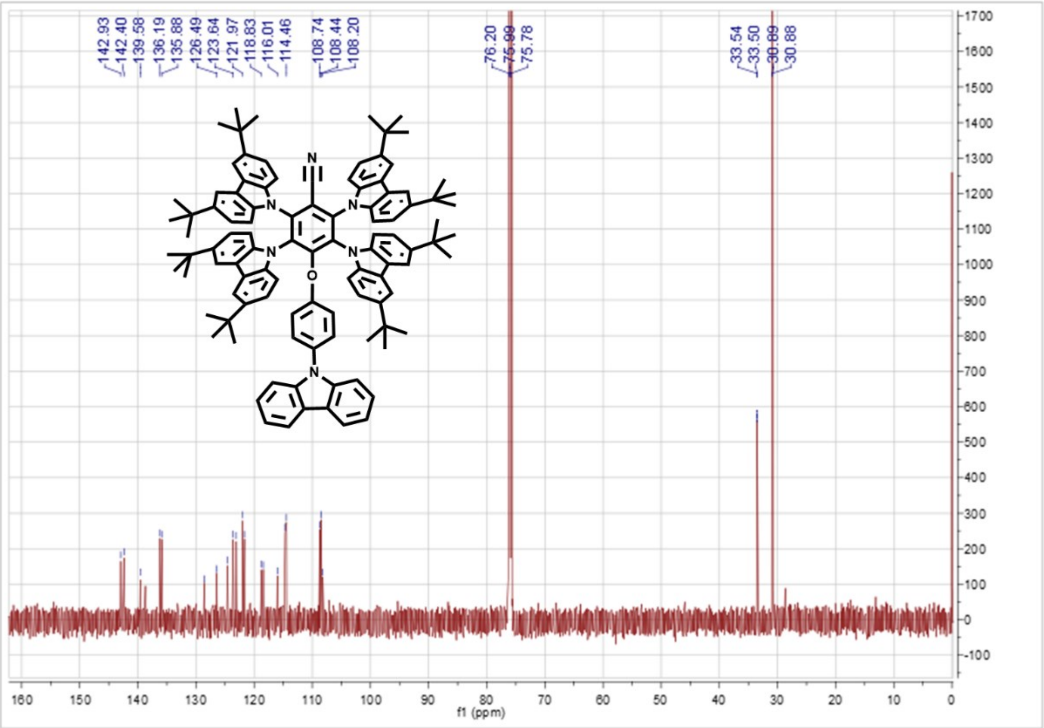
142.93
142.40
139.58
136.19
135.88
126.49
123.64
121.97
118.83
116.01
114.46
108.74
108.44
108.20
76.20
75.99
75.78
33.54
33.50
30.89
30.88
N
O
1700
1600
1500
1400
1300
1200
1100
1000
900
800
700
600
500
400
300
200
100
0
-100
160
150
140
130
120
110
100
90
80
70
60
50
40
30
20
10
0
f1 (ppm)

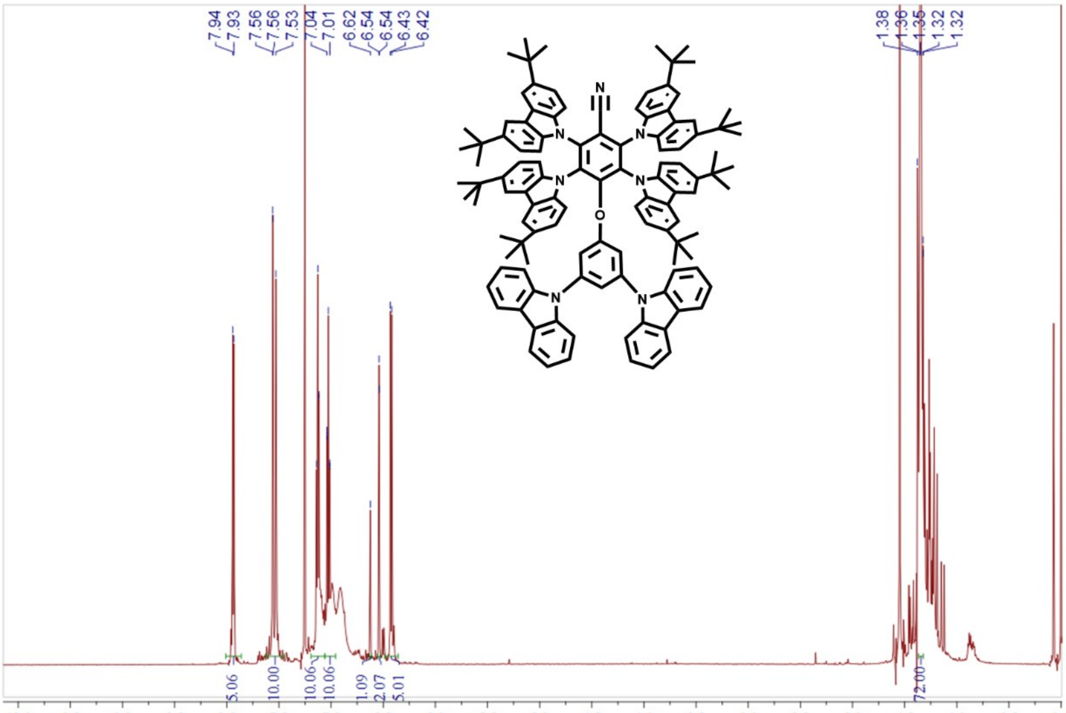
7.94
7.93
7.56
7.56
7.53
7.04
7.01
6.62
6.54
6.54
6.43
6.42
1.38
1.36
1.35
1.32
1.32
N
O
5.06
10.00
10.06
10.06
1.09
2.07
5.01
72.00
10.0
9.5
9.0
8.5
8.0
7.5
7.0
6.5
6.0
5.5
5.0
4.5
4.0
3.5
3.0
2.5
2.0
1.5
1.0
0.5
0.0
f1 (ppm)

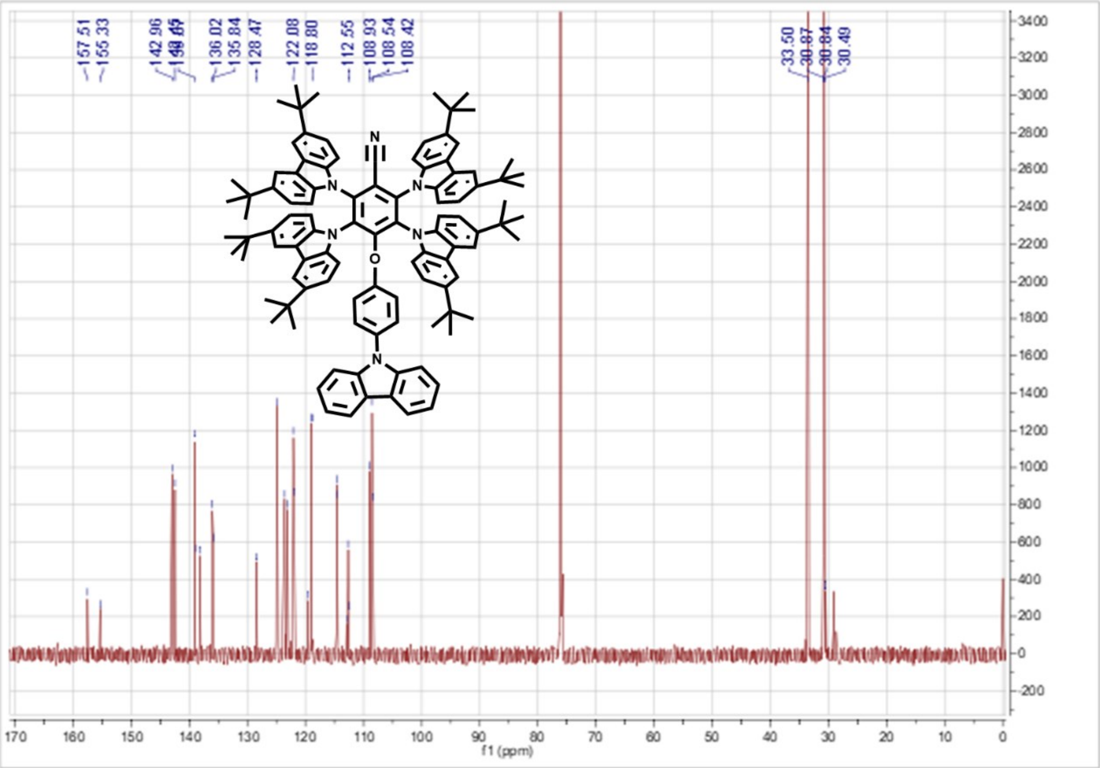
157.51
155.33
142.96
136.02
135.84
128.47
122.08
118.80
112.55
108.93
108.54
108.42
33.50
30.87
30.84
30.49
N
O
3400
3200
3000
2800
2600
2400
2200
2000
1800
1600
1400
1200
1000
800
600
400
200
0
-200
170
160
150
140
130
120
110
100
90
80
70
60
50
40
30
20
10
0
f1 (ppm)

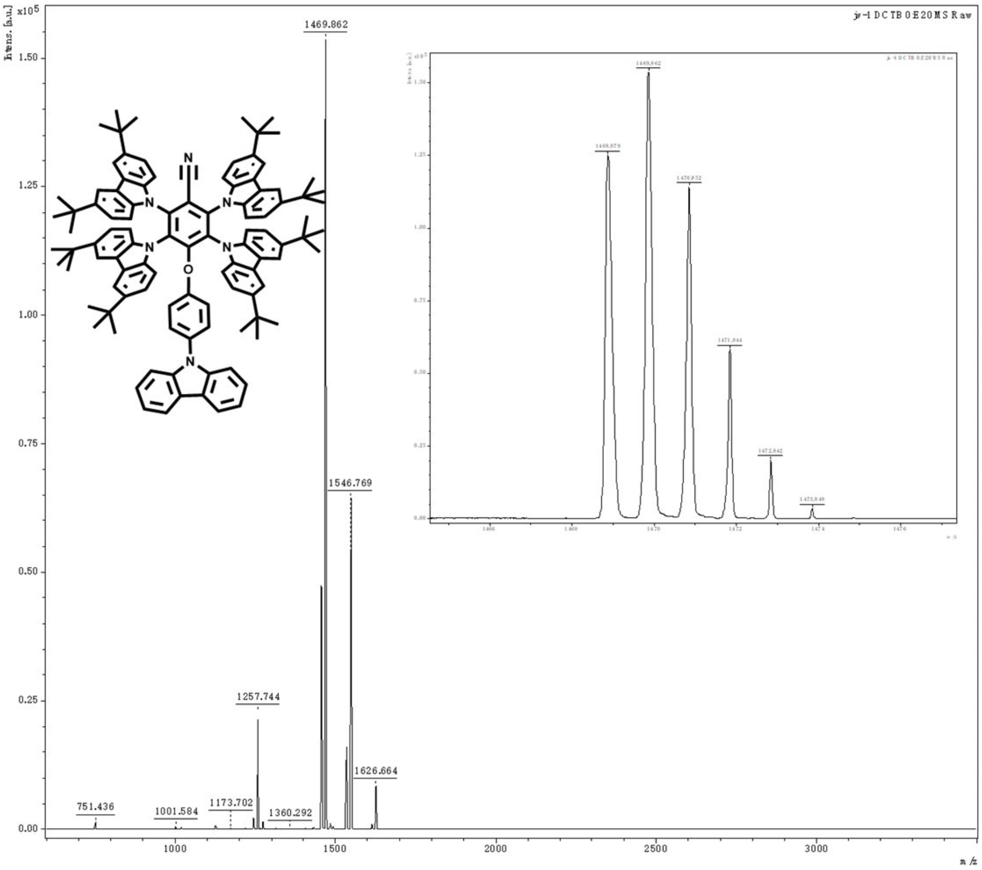
Intens. [a.u.]
x10^5
jw-1 DCTB 0E20MS Raw
1469.862
1546.769
1257.744
1626.664
751.436
1001.584
1173.702
1360.292
1468.879
1470.852
1471.844
1472.842
1473.848
1.50
1.25
1.00
0.75
0.50
0.25
0.00
1000
1500
2000
2500
3000
1466
1468
1470
1472
1474
1476
m/z
N
O

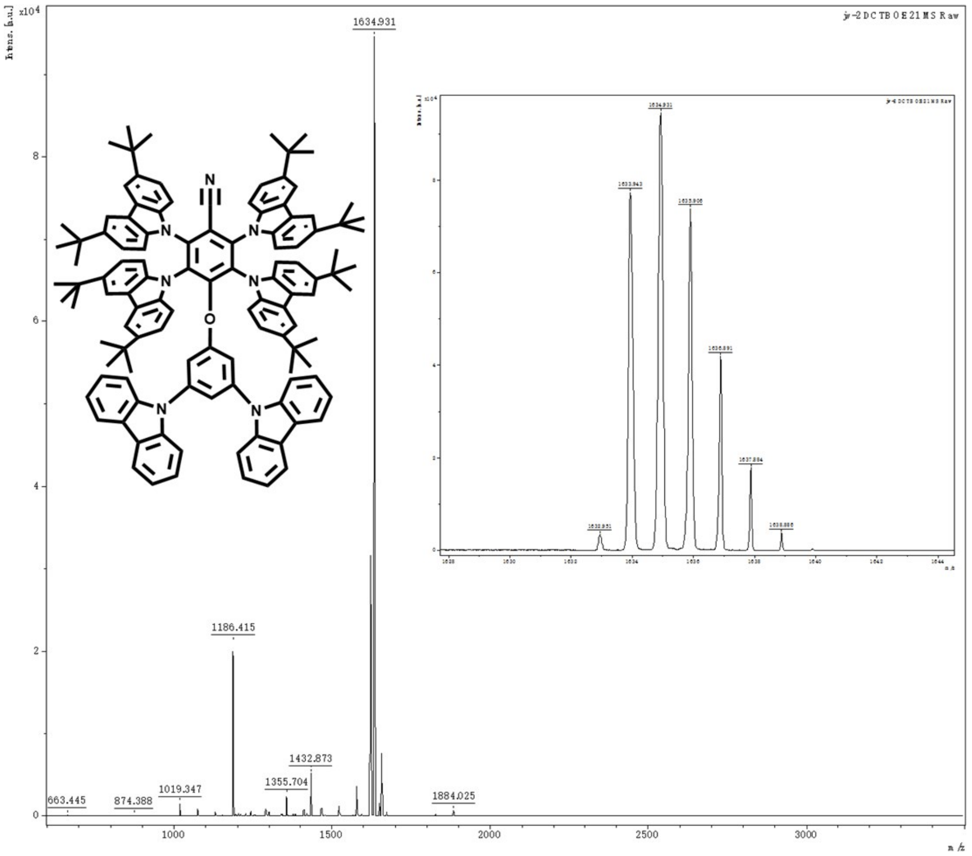

References

1. M. Watanabe, H. Hagiwara, Y. Ogata, A. Staykov, S. R. Bishop, N. H. Perry, Y. J. Chang, S. Ida, K. Tanaka and T. Ishihara, *J. Mater. Chem. A*, 2015, **3**, 21713-21721.
2. F. Wang, W. Qiu, J. Zeng, P. Yuan, W. Zong, W. Wu, Y. Liu, S. Xu, S.-J. Su and S. Cao, *J. Mater. Chem. C*, 2020, **8**, 4469-4476.
3. Z.-H. Zhao, H. Jin, Y.-X. Zhang, Z. Shen, D.-C. Zou and X.-H. Fan, *Macromolecules*, 2011, **44**, 1405-1413.
4. G. Zhao, D. Liu, W. Tian, W. Jiang and Y. Sun, *Dyes Pigm.*, 2020, **175**.
5. D. Zhang, M. Cai, Y. Zhang, D. Zhang and L. Duan, *Materials Horizons*, 2016, **3**, 145-151.